



TITLE:

A Gas Target System for Nuclear Scattering Experiments with Broad Range Magnetic Spectrograph

AUTHOR(S):

Matsuki, Seishi; Ogino, Kouya; Sakamoto, Naoki

CITATION:

Matsuki, Seishi ...[et al]. A Gas Target System for Nuclear Scattering Experiments with Broad Range Magnetic Spectrograph. Bulletin of the Institute for Chemical Research, Kyoto University 1985, 63(1): 40-46

ISSUE DATE:

1985-03-30

URL:

<http://hdl.handle.net/2433/77091>

RIGHT:

A Gas Target System for Nuclear Scattering Experiments with Broad Range Magnetic Spectrograph

Seishi MATSUKI*, Kouya OGINO**, and Naoki SAKAMOTO***

Received February 9, 1985

A gas target system for nuclear scattering experiments with broad range magnetic spectrograph was developed. The system consists of a cylindrical-type gas target chamber and double slits one of which was set on the rotating table in a scattering chamber. The rear slit was the entrance aperture itself of the broad-range magnetic spectrograph. The whole system was successfully checked by comparing the yields of protons from $^{12}\text{C}(p, p')$ scattering in gas target with in solid target. The system details and its performance are described.

KEY WORDS: Gas Target/ Nuclear Scattering/ Magnetic Spectrograph/

I. INTRODUCTION

Broad-range magnetic spectrographs have been extensively used recently for precise measurements of nuclear reactions. Recent development of high-resolution magnetic spectrograph enabled us to measure reaction products with an accuracy of 0.1%–0.01% energy resolution. In order to extend such precise measurements to nuclei of non-solid state such as rare gas, it is important to develop a gas target system which should be well suited for use with magnetic spectrograph, maintaining still a good energy resolution of the spectrograph.

Usually double slits (two apertures in parallel planes) are used for gas target to limit the effective target volume, resulting thus not a point target, but a line target¹⁾. The double slit system can be also used for broad-range magnetic spectrograph. Since, however, the magnetic spectrograph system, which usually consists of a couple of quadrupole and dipole magnets, has its own entrance aperture, this aperture should be used for the rear slit of the double slit system. We have developed such a double-slit gas-target system used for the magnetic spectrograph equipped to the FM cyclotron of the Institute for Nuclear Study, University of Tokyo. The gas target system has been successfully used for many experiments with various Kr and Ar isotopic gas targets.²⁻⁷⁾ In this note the system details and its performance are described.

II. APPARATUS

The gas target chamber used is of cylindrical-type made of stainless steel with 10 cm diameter. Havar foils of 2.5 μm thickness were used for both the beam entrance

* 松本征史: Laboratory of Nuclear Reaction, Institute for Chemical Research, Kyoto University, Kyoto.

** 萩野晃也: Department of Nuclear Engineering, Kyoto University, Kyoto.

*** 坂本直樹: Department of Physics, Nara Women's University, Nara.

A Gas Target System for Nuclear Scattering Experiments

and exit windows and also for the detection window of outgoing particles. The Havar foils were glued with epoxy-resin (araldite) on the stainless steel chamber and the glued area was covered with a thin brass sheet; this cover prevented the glued area of Havar foils from directly pulled outside by gas pressure, thus enabling the gas pressure to keep higher up to 500 mmHg. Inside the gas-target chamber, three lead blocks are inserted to reduce the inner volume of the chamber, thus enabling the use of the chamber efficiently for rare enriched isotopes as shown in Fig. 1.

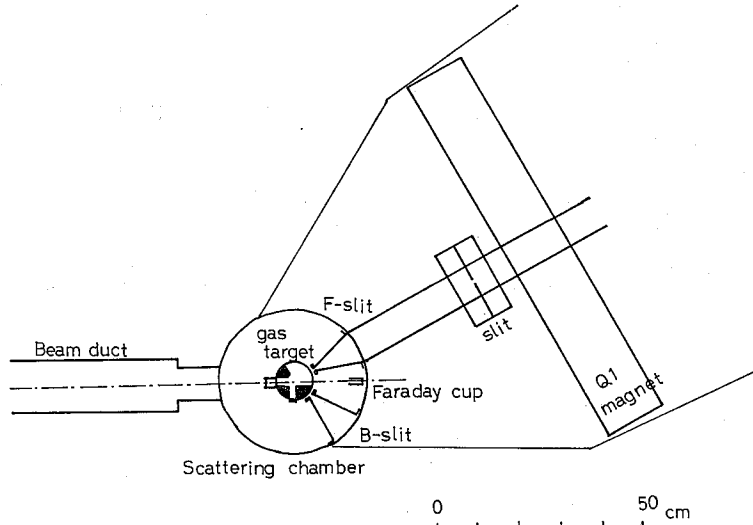


Fig. 1. Schematic plane view of the gas target system.

On the rotating table in the scattering chamber, two slits of 2 mm (F-slit) and 4 mm (B-slit) apertures, respectively, were set just in front of the window foil of the gas target chamber for the front slit as seen in Fig. 1. The narrow slit (F-slit) was used at forward angles to get better energy resolution than with the other slit of 4 mm wide (B-slit). The slit was made of 7 mm thick tantalum and the paths from the front slit to the inner wall of the scattering chamber were covered with 7 mm thick brass sheets to reject the outgoing particles entering into the spectrograph through this area.

A defining slit in front of the quadrupole magnet of the magnetic spectrograph⁸⁾ and the front slit on the rotating table define the solid angle of the magnetic spectrograph and also the line source area of the gas target. The distance between the front slit (on the rotating table) and the entrance slit on the spectrograph is 50 cm. The effective apertures of the spectrograph are 1.47 cm in horizontal and 6.00 cm in vertical, respectively⁸⁾. The effective length of the target is thus about 0.45 cm, and 0.90 cm, for F and B slits, respectively.

The gas handling system is shown in Fig. 2. To reduce the volume in the handling system, stainless steel pipes of 1 mm inner diameter were used to connect between valves, vacuum gauges and others. Since Kr gas can be solidified at liquid N₂ temperature, a reservoir made of stainless steel was incorporated between the gas

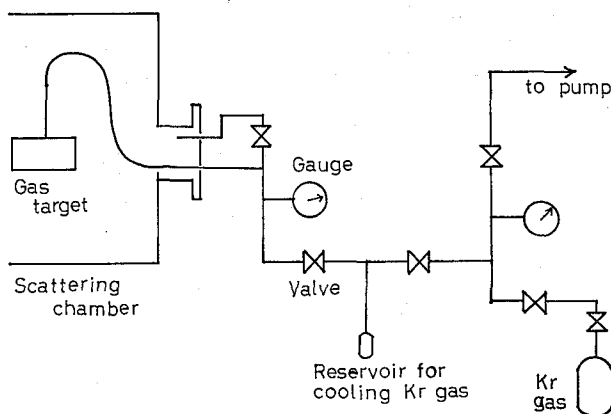


Fig. 2. Gas handling system especially designed for the Kr gas which was cooled by liquid N_2 and solidified to compress a small quantity of the enriched isotopic gas.

target and the Kr gas vessel to cool and solidify the Kr gas. This function worked well and enabled us to use efficiently a small quantity of enriched isotopes.

III. PERFORMANCE AND DISCUSSION

In order to know the solid-angle dependence on the detection angle and energy resolution of the detected particles, elastic and inelastic scattering of 52 MeV protons from ^{12}C were measured with the system; especially the yields from the solid ^{12}C target and from the CH_4 gas target were compared with each other. The thickness of the solid ^{12}C target was about 2 mg/cm^2 and the pressure of CH_4 gas in the target chamber was about 300 mmHg. The following formula was used in the evaluation of cross sections in the laboratory system with gas target;⁹⁾

$$(\frac{d\sigma}{d\Omega})_{\text{lab.}} = \frac{Y \sin \theta}{nNG},$$

where n , N , Y and θ are total number of bombarding particles, number of target nuclei per unit volume, the yield of scattered particles detected by focal-plane counter system and the detection angle of particles in the laboratory system, respectively. The factor G is the effective "G-factor", giving the geometrical dependence of the effective solid angle subtended by the double slit system. Analytical expressions of the G factor for various aperture geometry have been evaluated by a number of authors^{4,9)} up to the fourth order in $1/R_0$ where R_0 is the distance from the center of the target to the rear aperture. Schematic diagram in the present aperture system is shown in Fig. 3. With the parameters given in the figure, the factor G is given by⁹⁾

$$G = G_{00} \left[1 + d_0 + \frac{\sigma^{(1)}}{\sigma} d_1 + \frac{\sigma^{(2)}}{\sigma} d_2 + \dots \right],$$

where

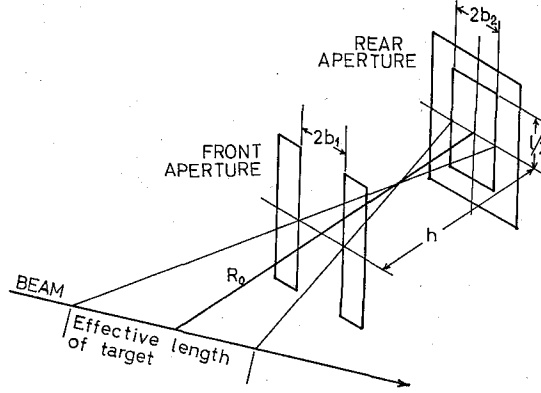


Fig. 3. Double slit geometry used in the present gas target system.

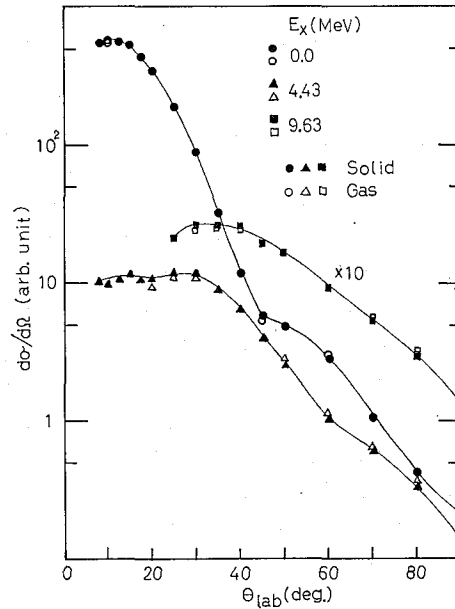
$$G_{00} = \frac{4b_1 b_2 l}{R_0 h},$$

$$A_0 = \frac{1}{3} \frac{\cos^2 \theta}{\sin^2 \theta} \frac{b_2^2}{R_0^2} - \frac{(b_1^2 + b_2^2)}{2h^2} - \frac{1}{8} \frac{l^2}{R_0^2},$$

$$A_1 = \frac{1}{3} \frac{\cos \theta}{\sin \theta} \left\{ \frac{l^2}{8R_0^2} - \frac{b_2^2}{R_0 h} \right\},$$

$$A_2 = \frac{1}{6} \frac{(b_1^2 + b_2^2)}{h^2},$$

and σ and $\sigma^{(n)}$ are the cross sections at θ and the n -th derivative of σ at θ , respectively. In the present system, the first term A_0 is less than 0.2% of the zeroth-


Fig. 4. Angular distributions of protons from the $^{86}\text{Kr}(p, p')^{86}\text{Kr}$ scattering leading to the 0^+ , 2^+ and 3^- states of ^{12}C .

order term G_{00} , so that up to A_0 is enough to take into account normally, consistent with the experimental result as shown below.

The angular distributions of protons leading to the ground, the first (2^+ , 4.43 MeV) and the third excited (3^- , 9.63 MeV) state of ^{12}C are shown in Fig. 4, where both the data taken with solid ^{12}C target and with CH_4 gas target are shown together for comparison. As seen in the figure, the cross sections with the gas target are in good agreement with those with solid target, justifying the procedure to evaluate cross sections with the above formula.

Typical momentum spectrum of protons from the $^{86}\text{Kr}(p, p')$ scattering is shown in Fig. 5. The overall energy resolution for the elastic peak was about 130 keV at

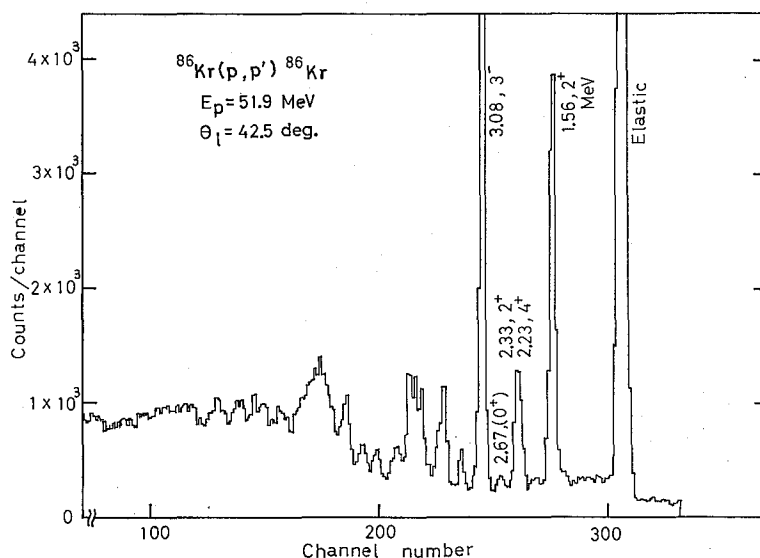


Fig. 5. Typical momentum spectrum of protons from the $^{86}\text{Kr}(p, p')^{86}\text{Kr}$ scattering measured in the present gas target system.

30°. This value is larger than that in the usual solid target, which is typically 80 keV. The most important contribution to the spread of the energy resolution is due to the finite line target in the gas target experiment. This can be seen in the following analysis; in the first-order theory of the beam transport, each element of beam transport and particle analysis system is expressed by a transfer matrix.¹⁰⁾ The effect of the finite (line) target volume is also expressed by a transfer matrix which transforms the incident particle vector into a scattered particle one. The coordinate system of this transfer is shown in Fig. 6 where θ is the detection angle of particles and coincides with the angle of the magnetic spectrograph. From this figure the vector of the incoming particle \mathbf{x}_1 is transferred to the scattered one \mathbf{x}_2 as¹¹⁾

$$\begin{pmatrix} x_2 \\ x_2' \end{pmatrix} = \begin{pmatrix} -\cos \theta & -S \cos \theta \\ 0 & 1 \end{pmatrix} \begin{pmatrix} x_1 \\ x_1' \end{pmatrix} + \begin{pmatrix} S \sin \theta \\ \theta - \beta \end{pmatrix}$$

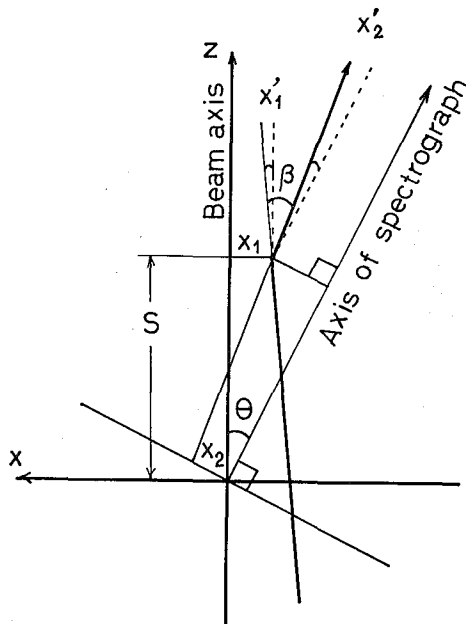


Fig. 6. Geometry of the scattered particles in the line source of gas target. (x_1, x_1') and (x_2, x_2') represent the horizontal components of the position and angular divergence of the incident and scattered beam, respectively.

where S is the effective length of the target volume. Since S is inversely proportional to $\sin \theta$, the overall width Δx_2 which contributes to the target volume is constant determined by the acceptance angle of the double-slit system. As described before, the effective target length is 0.45 cm for the F-slit system. Since a beam spot size of 3 mm diameter on the solid target gives 70 keV contribution to the energy spread of the outgoing particles in this magnetic spectrograph,⁸⁾ the effective target length produces about 105 keV spread. On the other hand the energy spread of the incident beam is estimated to be 50 keV (0.1%). Other sources of the energy spread are the energy loss of the incident beam in the gas target and the energy straggling of the incident beam due to Harvar foils (entrance and detecting foils). These contributions are estimated to be totally 50 keV. Thus the overall energy resolution obtained in the experiment is consistent with the estimation of several sources for finite resolution.

IV. CONCLUSION

A gas target system consisting of the cylindrical gas chamber and double-slits, rear of which is the entrance aperture itself of the magnetic spectrograph, was constructed and has been successfully used for many experiments.²⁻⁷⁾ Optimum energy resolution obtained in the actual scattering experiment was about 130 keV, being tolerable value compared with the resolution of 70–80 keV in the solid target experiment. This resolution was found to be mainly due to the effective target length.

If the spread of the target length is not so large compared to the normal beam in the solid target (about 1.5 times wider than that of normal beam in the present case), the additional spread of the energy resolution should be tolerable in the actual experiments. It is noted therefore that such a gas target system could also be usable for the higher-resolution magnetic spectrometers which give almost 0.02% energy resolution routinely at 50–100 MeV incident beam energies¹²⁾.

ACKNOWLEDGMENTS

The authors would like to thank Dr. T. Tanabe, Dr. M. Yasue, Mr. Y. Kadota, and Mr. Y. Saito for valuable suggestions and kind help throughout the experiments.

REFERENCES

- (1) G. Breit, K. Thaxton and L. Eisenbud, *Phys. Rev.* **55**, 1018 (1939).
- (2) S. Matsuki, N. Sakamoto, K. Ogino, Y. Kadota, S. Hayashi, T. Tanabe, M. Yasue, H. Yokomizo and S. Kubono, *Proceedings of the INS Symposium on Nuclear Collectivity*, edited by Y. Shida (Tokyo, 23–25 Sep. 1976) p. 414.
- (3) S. Matsuki, N. Sakamoto, K. Ogino, Y. Kadota, Y. Saito, T. Tanabe, M. Yasue and Y. Okuma, *Phys. Lett.*, **72B**, 319 (1978).
- (4) N. Sakamoto, S. Matsuki, K. Ogino, Y. Kadota, T. Tanabe and Y. Okuma, *Phys. Lett.*, **83B**, 39 (1979).
- (5) S. Matsuki, N. Sakamoto, K. Ogino, Y. Kadota, T. Tanabe and Y. Okuma, *Nucl. Phys.*, **A-370**, 1 (1981).
- (6) S. Matsuki, K. Ogino, Y. Kadota, N. Sakamoto, T. Tanabe, M. Yasue, A. Yokomizo, S. Kubono and Y. Okuma, *Phys. Lett.*, **113B**, 21 (1982).
- (7) T. Higo, S. Matsuki, K. Ogino, Y. Kadota, N. Sakamoto and T. Tanabe, to be published.
- (8) K. Yagi, *Nucl. Instr. Meth.* **31**, 173 (1964); K. Yagi, H. Ogawa, Y. Ishizaki, T. Ishimatsu, J. Kokame and K. Matsuda, *Nucl. Instr. Meth.* **52**, 29 (1976).
- (9) E. A. Silverstein, *Nucl. Instr. Meth.*, **4**, 53 (1959).
- (10) See for example, D. L. Hendrie, *Nuclear Spectroscopy and Reactions*, Part A, edited by J. Cerny (Academic Press, New York and London, 1974), p 366, and references cited therein.
- (11) See Ref. 10) for the definitions of the parameters used.
- (12) H. Ikegami, S. Morinobu, I. Katayama, M. Fujiwara and S. Yamabe, *Nucl. Instr. Meth.*, **175**, 335 (1980).